

nonmagnetic impurities this integral equation is given by 12:(A7), while for impurities with spin which exchange-scatter, Abrikosov and Gor'kov have shown that the integral equation becomes Ref. 23 Eq. (19) [to be denoted 23:(19)]

$$Q_{\omega}(\mathbf{p}, \mathbf{q}-\mathbf{p}) = \bar{G}_{\omega}(\mathbf{p}) \bar{G}_{-\omega}(\mathbf{q}-\mathbf{p}) \left[1 + n(2\pi)^{-3} \int d^3 p' \times (|u_1|^2 - |u_2|^2) Q_{\omega}(\mathbf{p}', \mathbf{q}-\mathbf{p}') \right]. \quad (\text{A4})$$

The impurity concentration is n , while u_1 and u_2 are the spin-independent and spin-flip scattering amplitudes, respectively. The one-electron propagator is [23:(14)]

$$\bar{G}_{\omega}(\mathbf{p}) = [i\omega - (\mathbf{p}^2/2m) + \mu + i \operatorname{sgn}\omega/2\tau], \quad (\text{A5})$$

and we introduce the scattering times

$$1/2\tau \equiv \pi n N(0) (|u_1|^2 + |u_2|^2), \quad (\text{A6})$$

$$1/2\tau_s \equiv \pi n N(0) |u_2|^2 \ll 1/2\tau.$$

Since u_1 and u_2 are assumed to be constants, Eq. (A4)

may be solved trivially; substituting into Eq. (A3) leads to

$$A(\mathbf{q}) = T \sum_{\nu} R(q) / [1 - n(|u_1|^2 - |u_2|^2) R(\mathbf{q})], \quad (\text{A7})$$

where

$$R(\mathbf{q}) \equiv (2\pi)^{-3} \int d^3 p \bar{G}_{\omega}(\mathbf{p}) \bar{G}_{-\omega}(\mathbf{q}-\mathbf{p}). \quad (\text{A8})$$

Substituting expression (A5) into (A8), the evaluation of $R(\mathbf{q})$ can be carried out, yielding [12:(A11)]

$$R(\mathbf{q}) = (2\pi N(0)/\nu_F q) \tan^{-1}(\nu_F q / [2|\omega| + (1/\tau)]). \quad (\text{A9})$$

For dirty materials where $q l \ll 1$, we may expand $R(\mathbf{q})$; substituting into Eq. (A7) leads to

$$Q(\mathbf{q}) = N(0) \left\{ \ln \frac{1.14 \Theta_D}{T} - \chi \left(\frac{q^2 \nu_F l}{6\pi\tau} + \frac{1}{2\pi T \tau_s} \right) \right\}. \quad (\text{A10})$$

Comparing Eq. (A10) with the previous analysis of Werthamer¹² in the nonmagnetic case completes the derivation of Eq. (7) in the text.

Optical Second-Harmonic Generation Using a Focused Gaussian Laser Beam*

J. E. BJORKHOLM

Microwave Laboratory, Stanford University, Stanford, California

(Received 27 September 1965)

This paper reports analytical and experimental results on optical second-harmonic generation in the focus of the lowest order transverse mode of a cw gas laser beam. The results of the calculation are explained in physical terms and are confirmed by experiments carried out in crystals of ammonium dihydrogen phosphate (ADP). The dependence of the second-harmonic power generated in a negatively birefringent crystal upon the crystal double-refraction angle and the divergence, or diffraction, of the focused beam is obtained. There are found to be four distinct asymptotic regions, determined by the ratios of the characteristic lengths z_R and l_a to the crystal length l , where the Rayleigh range of the focused beam z_R characterizes the focus, and l_a is characteristic of the crystal double-refraction angle α and the laser beam focal spot size w_0 . Proceeding from weak focusing to strong focusing (or in the direction of decreasing w_0), the second-harmonic power in the four regions varies as l^2/w_0^2 , $l/\alpha w_0$, w_0/α , and w_0^2 , respectively. There is an optimum degree of focusing, determined only by the crystal length, for which a maximum amount of second-harmonic power is generated. This degree of focusing corresponds to $z_R = l/\pi$, and the corresponding power which is generated depends upon both l and α . Optimum focusing in a crystal of ADP 1 cm long yields about 400 times more second-harmonic power than the collimated laser beam. The excellent agreement between analysis and experiment allows the accurate measurement of optical nonlinearities using focused beams. The results for the general case of a crystal anywhere along the focused beam are also presented. Interpretation of them shows that the limiting of second-harmonic generation by double refraction is determined by beam divergence, not beam radius.

I. INTRODUCTION

NONLINEAR optical effects are most readily detected when brought about by a beam of high-intensity light. For this reason, high-power Q -switched

ruby lasers and focused laser beams are often used in the study of such effects. In many cases, however, it is desirable to observe the nonlinear effects on a continuous basis. This necessitates the use of cw lasers, which are characterized by low power and hence low efficiency in inducing the desired nonlinear effects. For the case of optical second-harmonic generation (SHG), the technique of index matching must be employed in order to

* This work was supported by the Air Force Office of Scientific Research, United States Air Force, under Contract AF 49(638)-1525. The author is grateful to the Ground Systems Group of Hughes Aircraft Company for support furnished by a Hughes Doctoral Fellowship.

continuously generate measureable amounts of second-harmonic power. Focusing of the cw laser beam can be used to further enhance the conversion efficiencies and to allow measurement of smaller nonlinearities than otherwise would be possible on a cw basis.

This paper reports analysis and experiments on the generation of optical second harmonics in the focus of the Gaussian lowest order transverse mode of a continuous gas laser in negatively birefringent crystals. In particular, the aims of this paper are to obtain a precise expression for the amount of SHG obtained in the focus and to explain the results in physical terms; experimental results verify the analysis. An optimum degree of focusing is determined which can be employed to greatly enhance the conversion efficiencies obtainable from a given crystal. It is anticipated that similar calculations can be applied in a fairly direct fashion to consideration of other nonlinear processes which can be enhanced through the use of focusing.

The theory of the generation of optical second harmonics for idealized plane wave laser beams has been worked out in detail by Kleinman,¹ by Boyd, Ashkin, Dziedzic, and Kleinman (BADK),² and by Armstrong, Bloembergen, Ducuing, and Pershan (ABDP).³ ABDP consider the problem from the viewpoint of parametric interactions. This approach is particularly useful for the case of SHG by high-power pulsed ruby lasers since it adequately describes the case for which a significant portion of the fundamental beam is converted into the second harmonic. The theory as developed by Kleinman and BADK applies to the case of negligible conversion, so that the nonlinear polarization at twice the fundamental frequency, which is induced by the laser beam, may be viewed as a prescribed source giving rise to the second-harmonic wave. It is this viewpoint which will be applied in this paper.

In order to understand SHG in a focus, it is necessary to consider both the detailed shape of the laser beam and the birefringent properties of the crystal in which the second harmonics are being generated. Because the laser beam is finite in extent, it may be represented as a sum of many plane waves, or Fourier components, and because it is focused, the beam intensity is not uniform throughout the crystal. This latter fact means that the nonlinear polarization will be significant only within a limited region near the focus. For strongly focused beams this region will be much shorter than the crystal length; in such a case, only a portion of the crystal is effective in generating second-harmonic power. This limitation on SHG depends only upon the laser-beam geometry and is independent of the properties of the crystal medium.

Crystal birefringence also becomes important when

the index-matching technique is employed. Inasmuch as a real laser beam may be viewed as a sum of plane waves having a distribution of propagation directions, the effect of crystal birefringence makes it impossible for all plane wave components to be perfectly matched for optimum interaction. This leads to limiting of SHG by crystal double refraction and beam divergence.⁴ An alternative way of looking at this phenomenon is to realize that interaction between the fundamental and second-harmonic waves takes place along the direction of energy propagation for the second harmonic. However, because this wave is extraordinary, the direction of its Poynting's vector is different from that of the fundamental, and double refraction limits the distance over which the two beams can overlap. This was originally called the finite aperture effect by Kleinman,¹ but was more appropriately renamed the effect of double refraction in experimental and theoretical work by BADK.² In Sec. IV it is shown that these two points of view are equivalent only for columnar laser beams, those having a constant radius and planar phase fronts. For the general case in which the crystal is not restricted to the near field of the laser beam, it is shown that the effect of beam divergence upon index matching is the more fundamental point of view.

II. ANALYSIS

A. Calculation of Nonlinear Polarization

Consider the lowest order transverse mode of a gas laser to be focused in the center of a crystal capable of generating second harmonics, as shown schematically in Fig. 1. In order to preserve simplicity in the calculations, assume that the crystal is negatively birefringent ($n_o > n_e$); then the fundamental beam is introduced as an ordinary ray to index match to the extraordinary second-harmonic wave. This is the case encountered with crystals of ammonium dihydrogen phosphate (ADP), potassium dihydrogen phosphate (KDP), and

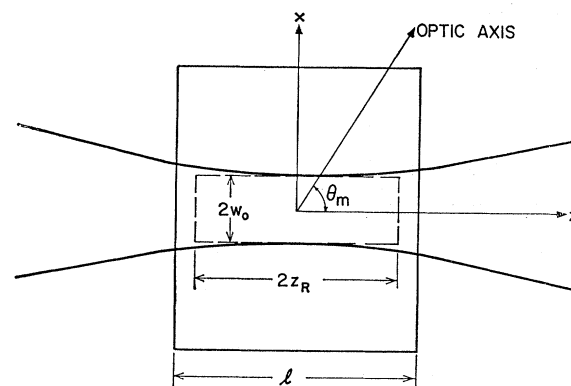


FIG. 1. Schematic diagram of the Gaussian laser beam focused in the center of the crystal. The cylindrical approximation for the focused beam is shown by the dashed figure.

¹ D. A. Kleinman, Phys. Rev. **128**, 1761 (1962).

² G. D. Boyd, A. Ashkin, J. M. Dziedzic, and D. A. Kleinman, Phys. Rev. **137**, A1305 (1965).

³ J. A. Armstrong, N. Bloembergen, J. Ducuing, and P. S. Pershan, Phys. Rev. **127**, 1918 (1962).

⁴ G. E. Francois and A. E. Siegman, Phys. Rev. **139**, A4 (1965).

calcite; ADP crystals were used in the experiments to be reported here. The laser beam is propagating along the z axis and is focused at the center of a crystal having length l . The incident and exit faces of the crystal are parallel and are cut so that at normal incidence the laser beam passes through the crystal in the index-matching direction, at an angle θ_m to the optic axis.

Description of the laser beam focused inside the crystal is a straightforward problem since the beam is an ordinary wave and the crystal appears as an isotropic medium to it. In the focal plane, at $z=0$, the optical electric field is polarized along the y axis and is given by

$$\mathbf{E}(x, y, z=0) = \hat{y} E_\omega \exp[-(x^2 + y^2)/w_0^2]. \quad (1)$$

The time dependence $e^{-i\omega t}$ has been suppressed in this equation. The beam focal spot size is w_0 ; it is defined as that radius at which the beam intensity falls to e^{-2} of its value on axis.

The optical electric field at other points inside the crystal is determined using Fourier analysis. That is, the focused beam is viewed as a sum of many plane waves, each propagating as $\exp[i(\mathbf{k} \cdot \mathbf{r} - \omega t)]$ in a distribution of directions around the z axis. Since each plane wave is an ordinary wave, the magnitude of the propagation vector \mathbf{k} is independent of direction:

$$k^2 = ((\omega/c)n_1^0)^2 \equiv k_1^2, \quad (2)$$

where n_1^0 is the index of refraction for the ordinary ray at the fundamental frequency ω , and c is the speed of light in vacuum. Fourier analysis of the focal plane distribution yields

$$\mathcal{E}(k_x, k_y, k_z)$$

$$= \hat{y} E_\omega (\frac{1}{2} w_0^2) e^{-w_0^2 k_T^2 / 4} \delta[k_z - k_1 (1 - k_T^2 / k_1^2)^{1/2}], \quad (3)$$

where $k_T^2 \equiv k_x^2 + k_y^2$ and $\delta(x)$ is the Dirac delta function. The introduction of the delta function, which relates k_z to k_T and k_1 , is an approximation inasmuch as there are values of $k_T > k_1$. This contradicts Eq. (2) and it means that the focal plane distribution Eq. (1) cannot be represented by strictly monochromatic plane waves. However, as long as the Fourier components associated with $k_T > k_1$ are very small, the Fourier inversion will be an extremely good approximation to the actual field. This requires

$$\frac{1}{2} k_1 w_0 \gg 1. \quad (4)$$

The aperture of the beam must be much greater than the wavelength of the light. The departure from strict monochromacy and the restriction on w_0 would also be required if Kirchoff's diffraction theory were applied.⁵ The restriction $k_1 w_0 / 2 \gg 1$ is equivalent to $k_T / k_1 \ll 1$. This relation will be used again in carrying out other steps of the analysis and is valid for cases of experimental interest. In particular, for SHG in ADP by light having a wavelength of 6328 Å, $k_1 = 1.51 \times 10^5 \text{ cm}^{-1}$ and Eq. (4) is satisfied for $w_0 \geq 10^{-4} \text{ cm}$. Further analysis will show

⁵ M. Born and E. Wolf, *Principles of Optics* (Pergamon Press, Ltd., London, 1964), Sec. 8.3.2.

that this range for w_0 , over which the analysis is valid, is also the range of experimental interest.

Inversion of Eq. (3) using approximations dependent upon the relation $k_T / k_1 \ll 1$ yields

$$\mathbf{E}(x, y, z) = \hat{y} E_\omega e^{i k_1 z} \times \frac{\exp\{-(x^2 + y^2)/w_0^2(1 + \xi^2)\}(1 - i\xi)}{1 + i\xi}, \quad (5)$$

where $\xi = 2z/k_1 w_0^2 \equiv z/z_R$. This is the expression for the electric field of the focused laser beam throughout the crystal. All details of the beam shape are specified by w_0 .

The electric field given by Eq. (5) is of the same general form as that which has been obtained using confocal resonator theory.^{6,7} The spot size of the beam is

$$w(z) = w_0(1 + \xi^2)^{1/2} \quad (6a)$$

and the radius of curvature of the surfaces of equal phase is

$$R(z) = z(1 + \xi^2)/\xi^2. \quad (6b)$$

The length parameter $z_R \equiv \frac{1}{2} k_1 w_0^2$ can be called the *Rayleigh range* of the focused beam, in analogy with antenna theory⁸; it is that value of z for which the power density on axis falls to $\frac{1}{2}$ of its value at the focal plane, or at which $w(z) = \sqrt{2} w_0$.

The dimensionless parameter ξ characterizes the various regions of the focused beam. The region for which $|\xi| \ll 1$ is called the *near field* of the focus. In this region the radius of the beam is essentially constant and the wave fronts of equal phase are nearly planar; the beam may be treated as columnar. The *far field* of the beam is that region for which $|\xi| \gg 1$. In this region the beam appears to be emanating from a point source on the axis at $z=0$. The half angular divergence of the beam is

$$\delta = 2/k_1 w_0, \quad (7)$$

Hence, Eq. (4) is equivalent to $\delta \ll 1$. From physical reasoning it can be asserted that $k_T / k_1 \lesssim \delta$. It is useful to mention a qualitative device which will help to understand the effects of beam shape upon SHG. Since the induced nonlinear polarization is proportional to the intensity of the laser beam, the most significant portion of the second-harmonic polarization will exist within z_R of the focal plane. As a result, a good qualitative feeling for the effects involved can be obtained by considering the focused beam to be a cylindrical beam of radius w_0 and length $2z_R$. Such an approximation is shown by the dashed figure in Fig. 1. In cases for which z_R is much less than the crystal length, this approximate picture predicts that only a small part of the crystal is effectively radiating second harmonics.

⁶ G. D. Boyd and J. P. Gordon, *Bell System Tech. J.* **40**, 489 (1962).

⁷ G. D. Boyd and H. Kogelnik, *Bell System Tech. J.* **41**, 1347 (1962).

⁸ J. F. Ramsay, *Space/Aeronautics R & D Handbook 1960-1961* (Conover-Mast Publications, Inc., New York, 1961).

The second-harmonic polarization induced in the crystal by the laser beam is related to the optical electric fields by⁹

$$p_i^{2\omega} = \chi_{ijk} E_j E_k, \quad (8)$$

when the Einstein summation convention is used. The i, j, k refer to the crystallographic axes and χ_{ijk} is the second-order nonlinear electric-susceptibility tensor element which gives rise to the second-harmonic polarization. In Eq. (8), $p_i^{2\omega}$ and E_j are the space-dependent amplitudes of the polarization and optical electric fields having a time dependence of $e^{-i2\omega t}$ and $e^{-i\omega t}$, respectively. When the technique of index matching is employed in negatively birefringent crystals, only the second-harmonic polarization having a component along the extraordinary-ray electric field will produce SHG. In ADP and KDP the component of interest is

$$p_{z'}^{2\omega} = 2d_{36} E_{x'} E_{y'} = d_{36} E_{\omega}^2, \quad (9)$$

where z' is the optic axis of the crystal and E_{ω} is the wave amplitude for the total ordinary laser beam ($E_{x'} = E_{y'} = E_{\omega}/\sqrt{2}$ for maximum efficiency). Second harmonics can also be generated in crystals of calcite if appropriate biasing dc electric fields are applied to destroy the center-of-symmetry of the crystal. This effect is called electric-field-induced SHG (ESHG).⁹ For calcite, one of the polarization components effective in SHG is given as

$$p_{z'}^{2\omega} = -\chi_{z'y'y'} E_{y'}^0 E_{y'} E_{y'} = -\chi_{51} E_{y'}^0 E_{\omega}^2, \quad (10)$$

where $E_{y'}^0$ is the biasing field.

In carrying out the analysis, the general form

$$p_{z'}^{2\omega} = \chi E_{\omega}^2 \quad (11)$$

is used in order to apply the end result to different crystals in a straightforward manner. Thus, the component of polarization effective in generating second harmonics in a focused beam is

$$p_{z'}^{2\omega} = \chi E_{\omega}^2 e^{2ik_1 z} (1+i\xi)^{-2} \exp\left[-2\frac{x^2+y^2}{w_0^2(1+i\xi)}\right]. \quad (12)$$

B. Calculation of the Second Harmonics Generated

To calculate the second-harmonic field which is generated, the second-harmonic polarization given in Eq. (12) will be decomposed into a sum of polarization plane waves via Fourier analysis. Making use of the results obtained by Kleinman¹ and BADK,² a growing second-harmonic wave can be associated with each polarization plane wave. The total second-harmonic field generated by the focused laser beam is obtained by summing these second-harmonic waves using Fourier inversion. Although this approach may appear involved, it is quite straightforward and it does make use of the well investigated theory of SHG by plane waves.

⁹ P. A. Franken and J. F. Ward, Rev. Mod. Phys. 35, 23 (1963).

The following transform pair is used:

$$p_{z'}^{2\omega}(\mathbf{r}) = \int_{-\infty}^{\infty} P_{z'}(\mathbf{K}) e^{i\mathbf{K}\cdot\mathbf{r}} d^3K \quad (13a)$$

and

$$P_{z'}(\mathbf{K}) = \frac{1}{(2\pi)^3} \int_{-\infty}^{\infty} p_{z'}^{2\omega}(\mathbf{r}) e^{-i\mathbf{K}\cdot\mathbf{r}} d^3r. \quad (13b)$$

The Fourier transform of Eq. (12) is

$$P_{z'}(\mathbf{K}) = (\chi E_{\omega}^2 / 16\pi) k_1 w_0^4 e^{-(2k_1 - K_z) k_1 w_0^2 / 2} \quad \text{for } (2k_1 - K_z) k_1 \geq \frac{1}{4} K_T^2 \geq 0 \\ = 0 \text{ otherwise,} \quad (14)$$

where $K_T^2 \equiv K_x^2 + K_y^2$.

The theory of second-harmonic generation by plane waves can now be applied. Inasmuch as this theory is rather involved, only those features of immediate use in the calculations will be discussed. The reader is referred to Ref. 2 for a concise summary of the theory and to Ref. 1 for the original work.

Each polarization plane wave gives rise to a growing second-harmonic wave. Each of these waves consists of a *forced* electric field plane wave, driven by the polarization and propagating as $e^{i\mathbf{K}\cdot\mathbf{r}}$, and a *free* plane wave, chosen in order to satisfy the boundary conditions at the entrance face of the crystal and propagating with a phase velocity appropriate to light at 2ω . The second-harmonic wave grows with distance because of constructive interference between these two plane waves; the interference remains constructive over a long distance when the forced and free waves have nearly the same phase velocity. This, of course, is why the technique of index-matching is used. The free plane waves are of the form

$$E_1 \hat{U} \exp(i2\omega n_2 \xi \cdot \mathbf{r}/c), \quad (15)$$

where $\hat{U} = \hat{U}(\xi)$ is a unit vector specifying the polarization of the free extraordinary wave, ξ is the unit vector in the direction of phase propagation, and $n_2 = n_2(\xi)$ is the index of refraction for the extraordinary wave of frequency 2ω propagating in direction ξ . Defining

$$\mathbf{K} = (2\omega/c) n' \hat{\sigma}, \quad (16)$$

where $\hat{\sigma} = \mathbf{K}/|\mathbf{K}|$ and n' is an effective index of refraction for the forced wave, the boundary conditions at the entrance face of the crystal are satisfied if

$$n' \hat{\sigma} - n_2 \xi = \varphi_{\mathbf{K}} \hat{N}, \quad (17)$$

where \hat{N} is the direction unit vector normal to the crystal face and $\varphi_{\mathbf{K}}$ is called the mismatch function. The result of these considerations is that each polarization plane wave

$$\mathbf{p}_{\mathbf{K}}(\mathbf{r}) = \mathbf{P}(\mathbf{K}) e^{i(\mathbf{K}\cdot\mathbf{r} - 2\omega t)} \quad (18)$$

produces a growing second-harmonic wave given by

$$\mathbf{E}_{\mathbf{K}}(\mathbf{r}) = z' g(2i\psi_{\mathbf{K}}) \gamma_{\mathbf{K}} \cdot \mathbf{P}(\mathbf{K}) e^{i(\mathbf{K}\cdot\mathbf{r} - 2\omega t)}, \quad (19)$$

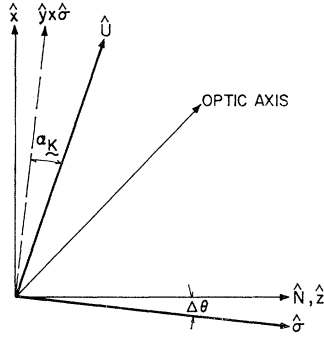


FIG. 2. The relationships between the various directions in a negatively birefringent crystal.

where $z' = z + \frac{1}{2}l$ and is the distance from the incident face of the crystal,

$$g(x) = (1 - e^{-x})/x = \int_0^1 e^{px} dp,$$

$$2\psi_K = 2 \frac{\omega}{c} \varphi_K z',$$

$$\gamma_K = 4\pi i \frac{\omega}{n_2 c} [\hat{N} \cdot \hat{\sigma} - (\hat{N} \cdot \hat{U})(\hat{\sigma} \cdot \hat{U})]^{-1} \hat{U} \hat{U}.$$

The integral representation for $g(x)$ is particularly useful for the calculations being carried out.

The relationships given here are exact, and judicious approximations are required to apply them to the problem at hand. In particular, both φ_K and γ_K are complicated functions of $\hat{\sigma}$; however, their dependence on propagation direction is greatly simplified by using $K_T/K_z \approx \delta \ll 1$. The manner in which $\gamma_K \cdot \mathbf{P}(\mathbf{K})$ varies with $\hat{\sigma}$ is demonstrated in Fig. 2. The angle α_K is called the angle of double refraction and is the angle between the directions of phase and energy propagation for an extraordinary ray. Clearly, the relationship is

$$\gamma_K \cdot \mathbf{P}(\mathbf{K}) = 4\pi i \frac{\omega}{n_2 c} \hat{U} P_{z'}(\mathbf{K}) \times \frac{\sin(\theta m + \alpha_K + \Delta\theta)}{\cos^2 \alpha_K \cos \Delta\theta - \frac{1}{2} \sin 2\alpha_K \sin \Delta\theta}. \quad (20)$$

The variation with $\Delta\theta$ is small for small changes of $\Delta\theta$ around zero. In particular, estimate $\Delta\theta \lesssim K_T/K_z \lesssim 2/k_1 w_0$ in agreement with the far-field divergence of the focused laser beam. For $w_0 \geq 6 \times 10^{-4}$ cm, $\Delta\theta$ will be on the order of one degree at most, and the variation of $\gamma_K \cdot \mathbf{P}(\mathbf{K})$ over such a small range can be neglected. Thus, Eq. (20) is approximated by

$$\gamma_K \cdot \mathbf{P}(\mathbf{K}) \approx 4\pi i \frac{\omega}{n_1^0 c} P(\mathbf{K}) \frac{\sin(\theta m + \alpha)}{\cos^2 \alpha} \hat{U}, \quad (21)$$

where α is the angle of double refraction for an extraordinary ray passing through the crystal in the index-matching direction.

The approximation used to simplify φ_K is straight-

forward. From Eq. (17) one obtains

$$\varphi_K z' = \varphi_K \hat{N} \cdot \mathbf{r} = (n'_1 \sigma_z - n_2 s_z) z'. \quad (22)$$

The variation of n_2 with $\hat{\sigma}$ is accounted for using the fact that the focused beam is passing through the crystal in the index-matching direction:

$$n_2(\hat{\sigma}) \approx n_1^0 - \frac{\partial n_2}{\partial \theta} \bigg|_{\theta = \theta_m} \frac{s_x}{s_z} \approx n_1^0 (1 + \alpha K_x / K). \quad (23)$$

Use has been made of the relation²

$$\alpha \approx \tan \alpha = - \frac{1}{n_1^0} \frac{\partial n_2}{\partial \theta} \bigg|_{\theta = \theta_m}. \quad (24)$$

For negatively birefringent crystals, $\alpha > 0$. In the same vein, the approximation $s_T^2 = n_1^{02} \sigma_T^2 / n_2^2(\hat{\sigma}) \approx \sigma_T^2$ yields

$$s_z \approx 1 - K_T^2 / 8k_1^2. \quad (25)$$

Substituting the approximate relations of Eqs. (23) and (25) into Eq. (22) results in an evaluation of the mismatch function

$$2\psi_K \approx (K_z - 2k_1 - \alpha K_x) z' + (K_T^2 / 4k_1) z'. \quad (26)$$

The same result is obtained by BADK² in a more rigorous fashion.

The total second-harmonic electric field is calculated using Fourier inversion

$$\mathbf{E}_{2\omega} = \int_{-\infty}^{\infty} \mathbf{E}_K(\mathbf{r}) d^3 K,$$

and Eqs. (14), (19), (21), and (26). The result is conveniently expressed as

$$\mathbf{E}_{2\omega}(\mathbf{r}) = \hat{U}_0 E_{2\omega} e^{2ik_1 z} \frac{z'}{z_R + iz} \int_0^1 dp \times \frac{\exp\{-[k_1/(z_R + iz)][y^2 + (x + \alpha z' p)^2]\}}{(z_R + iz - ipz')}, \quad (27)$$

where

$$E_{2\omega} = \pi i k_1^2 w_0^4 \frac{\omega}{n_1^0 c} \chi E_{\omega}^2 \frac{\sin(\theta m + \alpha)}{\cos^2 \alpha}.$$

This equation, expressed in somewhat different form, was previously derived by McMahon and Franklin¹⁰ using a different approach. Their calculations were carried out by summing the radiation from the phased distribution of dipoles which the nonlinear polarization represents.

The exponential factor in the integrand of Eq. (27) explicitly demonstrates that the cumulative interaction

¹⁰ D. H. McMahon and A. R. Franklin, Appl. Phys. Letters 6, 14 (1965).

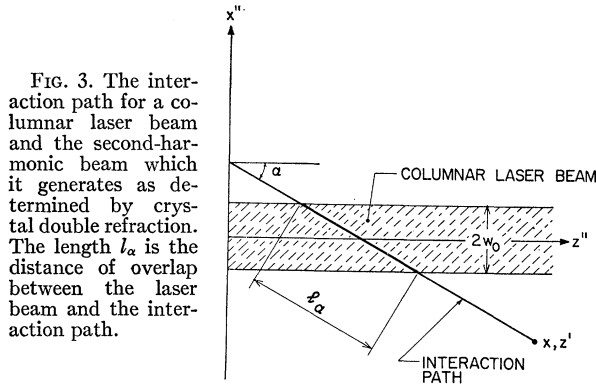


FIG. 3. The interaction path for a columnar laser beam and the second-harmonic beam which it generates as determined by crystal double refraction. The length l_α is the distance of overlap between the laser beam and the interaction path.

between the nonlinear polarization and the second-harmonic beam takes place along the direction of energy flow for the extraordinary second harmonic wave. It is apparent that the electric field at the point x, y, z' is determined by the polarization at the points x'', y'', z'' given by

$$\begin{aligned} y'' &= y, \\ z'' &= z'(1-p), \quad 0 \leq p \leq 1, \\ x'' &= x + \alpha z p. \end{aligned} \quad (28)$$

This path of interaction is shown in Fig. 3. Using the cylindrical approximation for a focused beam, it is clear that double refraction determines a maximum possible distance for coherent interaction (overlap) between the two beams. This distance is denoted by l_α and is proportional to w_0/α . For crystal lengths longer than l_α , SHG is limited by crystal double refraction. This analysis is not to be considered as general. In Sec. IV it will be shown that the reasoning applied here yields correct results only when calculating the maximum interaction length for columnar beams. The presence of double refraction has been verified in experiments by BADK.² Their measurements show that the transverse position of the peak of the generated second-harmonic beam does not coincide with that of the peak of the fundamental beam and that in lossless media it is displaced by an amount $\frac{1}{2}\alpha l$. McMahon and Franklin¹⁰ have demonstrated experimentally the effects of double refraction on the power generated by columnar beams.

The experimental work reported here is concerned with the dependence of the second-harmonic power generated, or the conversion efficiency, as a function of focal spot size, w_0 . Thus, it is desired to calculate the power transmitted by the second-harmonic beam across the x - y plane. In an anisotropic medium the \hat{z} component of the Poynting vector \mathbf{S} for a plane wave $\hat{U}E_{\mathbf{K}} \exp(i2\omega n_2(\hat{s})\hat{s} \cdot \mathbf{r}/c)$ can be written as²

$$\mathbf{S} \cdot \hat{z} = (c/8\pi) |E_{\mathbf{K}}|^2 n_2(\hat{s}) [\hat{s} \cdot \hat{z} - (\hat{z} \cdot \hat{U})(\hat{s} \cdot \hat{U})]. \quad (29)$$

A similar expression was discussed previously when considering the dyadic $\gamma_{\mathbf{K}}$ in Eq. (19). The same approximations used for $\gamma_{\mathbf{K}}$ can be applied to Eq. (29),

resulting in

$$\mathbf{S} \cdot \hat{z} \approx (n_1^0 c / 8\pi) |E_{\mathbf{K}}|^2 \cos^2 \alpha. \quad (30)$$

This equation is a valid approximation for plane-wave propagation in a direction near the z axis. Estimate also shows this to be a good point-by-point expression for the second-harmonic beam when $2/k_1 w_0 \ll 1$. Substitution of Eq. (27) into Eq. (30) and integration of the resulting expression over the x - y plane at the exit face of the crystal yields the total second-harmonic power

$$P_{2\omega} = \frac{128\pi^2 \omega^2}{n_1^0 s c^3} P_\omega^2 \frac{\sin^2(\theta m + \alpha)}{\cos^2 \alpha} \chi^2 \frac{l^2}{w_0^2} f(w_0, l, \alpha), \quad (31)$$

where

$$\begin{aligned} f(w_0, l, \alpha) &= \int_0^1 dp \int_0^1 dp' \\ &\times \frac{\exp[-(\alpha^2 l^2 / w_0^2)(p-p')^2]}{[1-i(l/z_R)(p-\frac{1}{2})][1+i(l/z_R)(p'-\frac{1}{2})]}. \end{aligned} \quad (32)$$

Use has been made of the fact that

$$E_\omega^2 = \frac{16 P_\omega}{n_1^0 c w_0^2} \quad (33)$$

and P_ω is the laser power. This basic result has also been obtained by McMahon and Franklin.¹⁰ They use a much different approach to the problem and analyze the result only for the case $l \ll w_0/\alpha \ll z_R$. For purposes of numerical calculation and for easier interpretation, it is convenient to express $f(w_0, l, \alpha)$ in terms of real quantities:

$$\begin{aligned} f(w_0, l, \alpha) &= \int_0^1 dp \int_0^1 dp' \\ &\times \frac{\left[1 + \left(\frac{l}{z_R}\right)^2 (p-\frac{1}{2})(p'-\frac{1}{2})\right] \exp\left[-\frac{\alpha^2 l^2}{w_0^2} (p-p')^2\right]}{\left[1 + \left(\frac{l}{z_R}\right)^2 (p-\frac{1}{2})^2\right] \left[1 + \left(\frac{l}{z_R}\right)^2 (p'-\frac{1}{2})^2\right]}. \end{aligned} \quad (34)$$

Equations (31), (32), and (34) are the desired expressions which describe the generation of optical second harmonics by a focused laser beam.

C. Asymptotic Solutions: Physical Significance

The dependence of the generated second-harmonic power upon the focal spot size w_0 , for fixed laser beam power, is displayed by

$$g(z_R, l, l_\alpha) \equiv (l^2/w_0^2) f(w_0, l, \alpha), \quad (35)$$

where $l_\alpha \equiv w_0/\alpha$ is the maximum distance for cumulative interaction between the fundamental and second-har-

monic beams as determined by crystal double refraction. Note that $f(w_0, l, \alpha)$ depends only on the ratios l/z_R and l/l_α ; in particular, the function displays four distinct types of asymptotic behavior.

In order to better understand the results which Eq. (35) will yield, the following qualitative argument is presented: The power generated in the second harmonic is proportional to the square of the nonlinear polarization, $\chi^2(P_\omega^2/w_0^4)$, times the approximate volume throughout which significant nonlinear polarization exists, $w_0^2 l_v$, times an "effective interaction length" l_c over which the cumulative interaction between the fundamental and second-harmonic beams occurs. Thus, for fixed P_ω ,

$$P_{2\omega} \propto g(z_R, l, l_\alpha) \propto (l_v l_c / w_0^2). \quad (36)$$

Depending on the relative sizes of w_0 and l , l_v will be either the crystal length l or twice the Rayleigh range of the focused laser beam, $2z_R$; l_c will be either l_v or the maximum interaction length l_α . Bearing this qualitative reasoning in mind, the four asymptotic regions are easily explained.

(i). $l \ll z_R$, $l \ll l_\alpha$: In this region the beam can be treated as columnar because $l \ll z_R$, and the effects of crystal birefringence can be neglected since $l \ll l_\alpha$. Equation (36) indicates that $g(z_R, l, l_\alpha) \propto l^2/w_0^2$. An exact expression for the limiting case $l \ll z_R$ can be found for Eq. (35):

$$g(z_R, l, l_\alpha) = \sqrt{\pi} \frac{l_\alpha}{w_0^2} \operatorname{erf} \frac{l}{l_\alpha} - \frac{l_\alpha^2}{w_0^2} (1 - e^{-l^2/l_\alpha^2}) \quad l \ll z_R. \quad (37)$$

The additional limit $l \ll l_\alpha$ applied to Eq. (37) yields

$$g(z_R, l, l_\alpha) = \frac{l^2}{w_0^2} \quad l \ll z_R, \quad l \ll l_\alpha. \quad (38)$$

In this limit, Eq. (31) becomes the well-known formula for second-harmonic generation by a plane wave in an "almost isotropic" medium.¹¹

(ii) $l_\alpha \ll l \ll z_R$: In this region, the laser beam remains plane wave in character, but crystal double refraction can no longer be neglected. The "effective interaction length" l_c is limited to l_α . Qualitatively, we expect

$$g(z_R, l, l_\alpha) \propto (l_\alpha / w_0^2) = l / w_0 \alpha. \quad (39)$$

Applying the limit $l_\alpha \ll l$ to Eq. (37), one obtains

$$g(z_R, l, l_\alpha) = \sqrt{\pi} (l / w_0 \alpha) \quad l_\alpha \ll l \ll z_R. \quad (40)$$

Thus, the exact analysis implies that for the case of double refraction-limited SHG, the correct choice for l_c is

$$l_c = l_\alpha' = \sqrt{\pi} (w_0 / \alpha). \quad (41)$$

(iii). $l_\alpha \ll z_R \ll l$: As the laser beam is focused more sharply, the beam spot size gets smaller and the point

is reached at which the beam diverges appreciably inside the crystal. It is noted that

$$z_R / l_\alpha = \frac{1}{2} \alpha k_1 w_0, \quad (42)$$

so that proceeding in the direction of decreasing w_0 , the case $l_\alpha \ll z_R$ occurs before the case $z_R \ll l_\alpha$ for nonzero values of α . Only a small part of the crystal is effectively radiating second harmonics. The qualitative prediction is

$$g(z_R, l, l_\alpha) \propto \frac{2z_R l_\alpha'}{w_0^2} = \sqrt{\pi} (k_1 w_0 / \alpha). \quad (43)$$

An exact solution for this asymptotic region has not been obtained from Eq. (34), but later can be found by analogy with the solutions for the other three asymptotic regions.

(iv). $z_R \ll l$, $z_R \ll l_\alpha$: The beam is now focused so sharply that crystal double refraction can be ignored. This case is the same as that of a sharply focused beam in an isotropic medium. Equation (36) predicts

$$g(z_R, l, l_\alpha) \propto (4z_R^2 / w_0^2) = k_1^2 w_0^2. \quad (44)$$

In this asymptotic region, solution of Eq. (34) gives

$$g(z_R, l, l_\alpha) = \frac{1}{4} \pi^2 k_1^2 w_0^2 \quad \begin{array}{l} z_R \ll l \\ z_R \ll l_\alpha \end{array}. \quad (45)$$

Equation (45) implies that the correct choice for l_v and l_c in this limit is

$$l_c, l_v = 2z_R' = 2(\frac{1}{2} \pi z_R) = \pi z_R. \quad (46)$$

This result allows a correct evaluation of the asymptotic solution for region (iii); namely

$$g(z_R, l, l_\alpha) = 2z_R' l_\alpha' / w_0^2 = \frac{1}{2} \pi^{3/2} (k_1 w_0 / \alpha). \quad (47)$$

$$l_\alpha \ll z_R \ll l.$$

The curves for the asymptotic solutions of $g(z_R, l, l_\alpha)$ as a function of w_0 take a particularly simple form on a log-log plot, as shown in Fig. 4. There are two different types of behavior, depending on the crystal length l . If

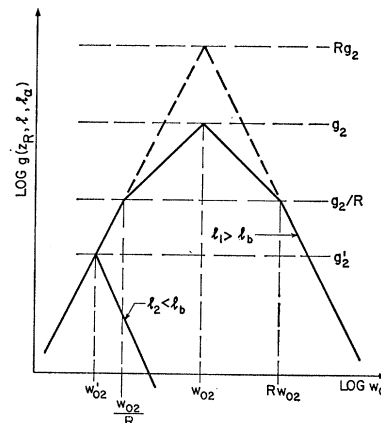


FIG. 4. The asymptotic solutions of $g(z_R, l, l_\alpha)$ for two crystal lengths. The values of the parameters which specify the curves are given in Eqs. (49) and (50).

¹¹ A. Ashkin, G. D. Boyd, and J. M. Dziedzic, Phys. Rev. Letters 11, 14 (1963).

l is small enough, regions (ii) and (iii) disappear. The requirement that the effects of double refraction vanish is $l < l_b$, where

$$l_b = 2/k_1\alpha^2. \quad (48)$$

This critical length l_b is 0.016 cm for crystals of ADP and 0.001 cm for calcite when using light at 6328 Å. Only for very short crystals of these materials will the effects of beam divergence or diffraction swamp out the effects of double refraction. It should be pointed out, however, that this is not meant to be a generalization and exceptions do exist. For instance, SHG can be brought about in long crystals of LiNbO₃ without any double-refraction effects.¹² This is because index matching for laser-beam propagation perpendicular to the optic axis can be accomplished in this crystal by adjusting the crystal temperature. For directions normal to the optic axis, $\alpha=0$ and l_b is infinite.

Depending on the relative size of l to l_b , the asymptotic curves in Fig. 4 are symmetric around either w_{02} or w_{02}' . The values of the important parameters for the two cases are given by

$$l_1 > l_b: \quad \begin{aligned} w_{02} &= (2l_1/\pi k_1)^{1/2}, \\ g_2 &= (\pi/\alpha)(\frac{1}{2}k_1 l_1)^{1/2}, \\ R &= \alpha(\frac{1}{2}k_1 l_1)^{1/2}, \end{aligned} \quad (49)$$

$$l_2 < l_b: \quad \begin{aligned} w_{02}' &= (2l_2/\pi k_1)^{1/2}, \\ g_2' &= \frac{1}{2}\pi k_1 l_2. \end{aligned} \quad (50)$$

Although these values are for the asymptotic curves, it is a reasonable assumption that the general over-all behavior of SHG in a focus can be gleaned from them. Thus, analysis shows that there is a maximum amount of second-harmonic power which can be generated in a given crystal of length l , for fixed laser power P_ω ; it is found that

$$\begin{aligned} [P_{2\omega}]_{\max} &\propto l \quad \text{for } l < l_b \\ &\propto l^{1/2} \quad \text{for } l > l_b. \end{aligned} \quad (51)$$

Figure 4 shows that a crystal in which there is no double refraction generates $R(\alpha)$ times as much second-harmonic power as a crystal of the same length having a double-refraction angle α . The analysis also indicates the optimum degree of focusing to be used. In particular, maximum second-harmonic power is obtained when

$$z_R = l/\pi \quad \text{or} \quad z_R' = \frac{1}{2}l. \quad (52)$$

Notice that optimum focusing is determined solely by the crystal length. Double refraction is not important in determining the value of w_{02} , but it does limit the maximum amount of power obtainable. This conclusion contradicts the statement given elsewhere¹¹ that the effects of coherence predominate over those of energy concentration. Indeed, the analysis here shows that

¹² R. C. Miller, G. D. Boyd, and A. Savage, Appl. Phys. Letters 6, 77 (1965).

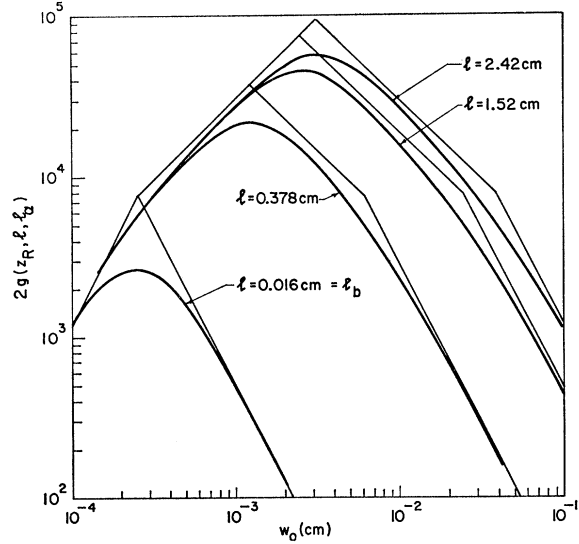


FIG. 5. Computed and asymptotic curves of $g(z_R, l, l_\alpha)$ for four crystal lengths of ADP, $\alpha=0.029$ rad.

energy concentration alone determines the optimum degree of focusing.

D. Exact Solution

Although the asymptotic solutions of $g(z_R, l, l_\alpha)$ are simple and instructive, exact solutions can also be obtained with the aid of an electronic computer. The heavy curves in Fig. 5 show computed solutions of $g(z_R, l, l_\alpha)$ for crystals of ADP, $\alpha=0.029$ rad, superimposed on the corresponding asymptotic curves.

III. EXPERIMENTAL MEASUREMENTS

The experimental setup shown schematically in Fig. 6 was used to verify the predictions of the analysis. The laser is a Spectra-Physics model 112 rf-excited helium-neon laser, operated at 6328 Å. The optical resonator was hemispherical, approximately 120 cm long, and was adjusted for oscillation only in the lowest order transverse mode. The operation was not single mode, how-

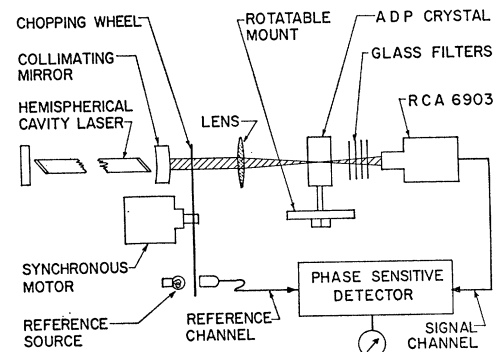


FIG. 6. Schematic diagram of the experimental setup.

ever, inasmuch as many longitudinal modes were present. Measurements carried out on this laser by Francois¹³ indicate that there is no self-locking¹⁴ of these modes. Thus it was assumed that the longitudinal modes were oscillating independently of one another. A so-called collimating mirror was used as the curved reflector. Due to the curvature of the back surface of this mirror, the beam transmitted by it has essentially plane phase fronts upon emerging. A typical beam radius for the output of the laser is 0.185 cm, meaning that the Rayleigh range of the collimated beam is very long, about 17 m. All experiments were conducted within 3 m of the laser.

A lens of focal length f was used to focus the laser beam at the center of an ADP crystal which was oriented in the index-matching direction. The crystals were cut so that the beam was within a few degrees of being normal to the entrance and exit faces at phase matching. After emerging from the crystal, the fundamental beam was strongly absorbed by four Corning CS7-54 glass filters. The second-harmonic beam passed through with slight loss to impinge on the photocathode of an RCA-6903 photomultiplier. This particular tube was chosen because its envelope is end-on to the light and its photocathode is large. The signal was detected by a Princeton Applied Research Corp. JB-5 lock-in amplifier, the laser beam being modulated at about 500 cycles/sec by a chopping wheel driven by a synchronous motor. The crystal holder was mounted on a rotatable disk and the angular orientation of the crystal accurately adjusted for maximum output, i.e., for proper index matching. The lenses were war surplus simple and achromatic compound coated lenses and ranged in focal length from 35 to 1016 mm. For longer focal lengths, a negative lens and a slightly stronger positive lens were used as a telephoto combination. Measurements made using such a combination lacked the accuracy obtained using a single lens because of mechanical jitter and errors in measuring the effective focal length. Accuracy problems were also encountered with short-focal-length lenses. The main difficulties were small lens aperture and the large divergence of the focused beams.

The experimental procedure required obtaining the correct axial and angular positioning of the crystal with respect to the focus of the laser beam. The correct location for the focus was obtained by sliding the lens along the optical bench until a maximum second-harmonic power output was recorded. This occurred when the focal spot coincided with the center of the crystal. When near-optimum focusing was used, the second-harmonic power fell off rapidly as the focal spot moved from the crystal center. For cases of much stronger or much weaker focusing, the changes were small. This behavior

is explained in terms of the size of the Rayleigh range of the focused beam relative to the crystal length. For weak focusing the laser beam is essentially a parallel or columnar beam, and the output is independent of where the crystal is located along the beam. For strong focusing most of the SHG occurs in the small focal region. The output is then essentially constant as long as the focus is inside the crystal, and negligible otherwise. With near-optimum focusing, strong SHG occurs in a focal region about as long as the crystal itself, so that the output drops if this region begins to move out of the crystal in either direction.

Using the techniques outlined here, the dependence of the second-harmonic power upon lens focal length and upon the radius of the collimated laser beam was obtained. The connection of these experimental results to the calculated results is established by calculating the focal spot size w_0' of a laser beam of radius W focused in air by a lens of focal length f . The result is

$$w_0' = \frac{W}{(1 + (k_0^2 W^4 / 4f^2))^{1/2}} \approx \frac{2f}{k_0 W}, \quad f \ll \frac{k_0 W^2}{2}, \quad (53)$$

where k_0 is the propagation constant for light in air. Equation (53) is a valid approximation for the experiments reported here. It can readily be shown that w_0' is still the spot size of the beam even when focused inside the crystal. Introduction of the crystal shifts the location of the focal spot in agreement with geometrical optics, but the spot size remains unchanged, $w_0 = w_0'$.

In the calculation of SHG in a focus, frequent use was made of the relation $2/k_1 w_0 \ll 1$. The values of w_0 used in the experiments, as calculated from Eq. (53), were such that $w_0 \geq 1.8 \times 10^{-4}$ cm and $k_1 w_0 / 2 \geq 13.5$. Thus all experimental measurements should be adequately described by the calculations carried out in this paper.

The radius of the collimated laser beam W was measured using a silicon solar cell mounted on a micromanipulator behind a 0.001-in.-diam. hole in an opaque screen. Initial measurements of W led to experimental curves which had the correct shape but which were displaced along the w_0 axis from the theoretical curves. It was later discovered that this discrepancy was due to the presence of laser oscillation at 6401 Å, as well as at 6328 Å, leading to false measurements of W . By isolating the 6328 Å line, the expected results were obtained.

Comparison of the experimental data with the calculated curves is shown in Figs. 7 and 8. Figure 7 shows the results for three different crystal lengths and approximately the same value of W . In Fig. 8 the results are shown for one crystal length and three different values of W obtained by expanding or contracting the laser beam diameter with the aid of normal or inverted telescopes. This technique introduced a good deal of mechanical jitter into the experiment and accounted for a loss of accuracy. The agreement between experimental

¹³ G. E. Francois (private communication).

¹⁴ M. H. Crowell, IEEE J. Quantum Electron., QE-1, 12 (1965).

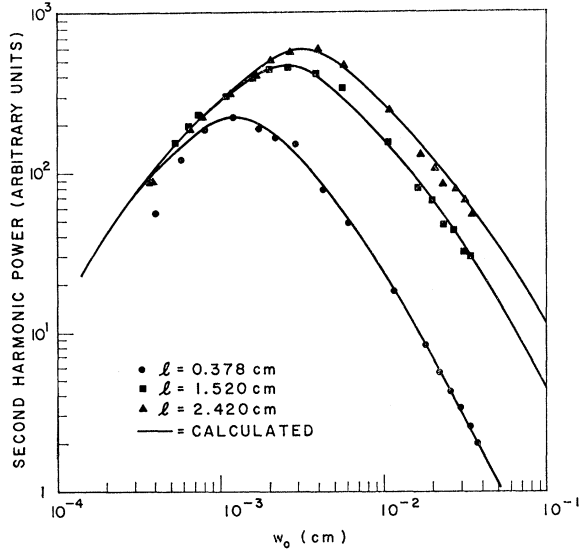


FIG. 7. Experimentally measured values of $P_{2\omega}/P_{\omega}^2$ compared with the computed curves of Eq. (35) for three crystals of ADP.

points and the computed curves is good enough that the results of the calculations can be considered as verified.

IV. LIMITING OF SHG BY DOUBLE REFRACTION AND BEAM DIVERGENCE

The general case of SHG anywhere along a focused laser beam is easily obtained from the analysis of Sec. IIB by redefining the parameter z' . Let the entrance face of the crystal be at $z=L$, the focal plane of the beam being at $z=0$. Also let the crystal be tilted away from the index matching direction by a small angle ϕ . This simply adds an additional term to the mismatch function used in the previous analysis. The result is

$$g(z_R, l, l_\alpha, \phi) = \frac{l^2}{w_0^2} \int_0^1 dp \int_0^1 dp' \frac{e^{-(\alpha^2 l^2 / w_0^2)(p-p')^2} e^{2ik_1 \alpha l \phi (p-p')}}{\left[1 + \frac{iL}{z_R} + \frac{il}{z_R}(1-p)\right] \left[1 - \frac{iL}{z_R} - \frac{il}{z_R}(1-p')\right]}. \quad (54)$$

This equation gives the dependence of the second-harmonic power upon position of the crystal along the focused beam and upon rotation of the crystal away from the index matching direction. In general, the dependence upon ϕ is not independent of L .

The meaning of Eq. (54) is most apparent in the limiting case $l \ll z_R$:

$$g(z_R, l, l_\alpha, \phi) = \frac{l^2}{w_0^2(1+L^2/z_R^2)} \int_0^1 dp \int_0^1 dp' \times e^{-(\alpha^2 l^2 / w_0^2)(p-p')^2} e^{2ik_1 \alpha l \phi (p-p')} \quad l \ll z_R. \quad (55)$$

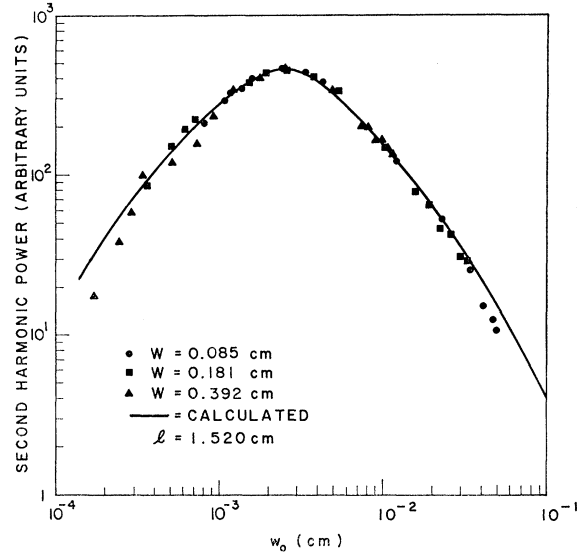


FIG. 8. Experimentally measured values of $P_{2\omega}/P_{\omega}^2$ compared with the computed curves of Eq. (35) for one crystal of ADP and three different collimated laser beam radii.

In this case the dependence of the second-harmonic power upon rotation of the crystal around the index-matching direction is independent of L . Using the relation

$$\frac{\sin^2 X}{X^2} = \int_0^1 dp \int_0^1 dp' e^{2iX(p-p')}, \quad (56)$$

Eq. (55) can be shown to be the same as the expression obtained by Francois and Siegman⁴ using a different method, namely

$$g(z_R, l, l_\alpha, \phi) = \frac{l^2}{w_0^2(1+L^2/z_R^2)} \frac{w_0}{\sqrt{\pi \alpha l}} \times \int_{-\infty}^{\infty} e^{-(w_0^2/\alpha^2 l^2)\psi^2} \frac{\sin^2(k_1 \alpha \phi + \psi)}{(k_1 \alpha \phi + \psi)^2} d\psi. \quad (57)$$

Their experiments verify this dependence upon both L and ϕ .

Equation (55) can yield better understanding of the fundamental processes involved in SHG by consideration of the case for $\phi=0$:

$$g(z_R, l, l_\alpha, 0) = \frac{l^2}{w_0^2(1+L^2/z_R^2)} \int_0^1 dp \times \int_0^1 dp' e^{-(\alpha^2 l^2 / w_0^2)(p-p')^2}. \quad (58)$$

The essential point is this. For a columnar beam of radius w we have concluded that the maximum possible interaction length (overlap) is w/α because of crystal double refraction. Equation (58) holds for $l \ll z_R$; in this case the beam radius is essentially constant inside the

crystal for all L . Even though the phase fronts of the beam are in general not planar, analogy tempts one to consider the maximum interaction length as w/α for this case too. However, in Eq. (58) it is clear that the appropriate interaction length is given by w_0/α , where w_0 is the beam radius at the focus, not at the crystal. The radius at the crystal is $w_0(1+L^2/z_R^2)^{1/2}$. Previous experiments which have demonstrated the effects of double refraction² were carried out with the crystal located in the focal region ($L \ll z_R$) of a beam for which $z_R \gg l$. Hence the distinction between w and w_0 was not significant. Thus the simple double-refraction point of view gives the correct maximum interaction length only for columnar beams, $L \ll z_R$. Extension of this viewpoint to beams having curved phase fronts is invalid.

It is better to regard the maximum interaction length as being determined by crystal double refraction and beam divergence instead of by double refraction and the beam radius at the crystal. A physical understanding can also be obtained for this point of view. The maximum interaction length l_α' for an extraordinary second-harmonic plane wave traveling at an angle δ , the beam divergence angle, to the optic axis can be defined as that value of z' for which the mismatch function, Eq. (26), is π rad:

$$l_\alpha' = \frac{1}{4}\pi(w_0/\alpha). \quad (59)$$

Thus limiting of SHG occurs because the presence of crystal double refraction means that it is impossible for all plane-wave components of the laser beam to be perfectly index-matched for optimum interaction. It is suggested that the length $l_\alpha = w_0/\alpha$ is most accurately referred to as the maximum interaction length as determined by crystal double refraction and beam divergence.

V. CONCLUSION

This paper has reported the analysis of optical SHG in the focus of a Gaussian laser beam and its substantiation by experiments carried out in crystals of ADP. The effects of crystal double refraction and beam divergence, or diffraction, were demonstrated by calculation and experiment. It is shown that these effects can be understood and expressed in terms of the ratios of the characteristic lengths z_R and l_α to the crystal length l . Diffraction effects are characterized by z_R and the effects of double refraction and beam divergence by l_α . An optimum degree of focusing exists and corresponds to

the case $z_R = l/\pi$. It is determined by the crystal length alone.

The use of focused beams can greatly enhance the generated second-harmonic power. For the experiments reported here optimum focusing in a crystal of ADP 1 cm long gives 400 times more power than the collimated laser beam. Enhancement is even greater for shorter crystals. However, it is to be stressed that the results reported here apply only to the case of negligible conversion of the fundamental into second harmonic, as is the case for cw laser beams. Focused beams can be used to measure smaller nonlinearities than otherwise could be possible on a cw basis.

The results for SHG anywhere along a focused beam were also presented. Discussion of these results led to a physical understanding of l_α in terms of the effects of double refraction upon the beam divergence, instead of upon the beam radius at the crystal. This was shown to be the more general point of view.

It is anticipated that the calculations and ideas presented can be extended to apply to other nonlinear processes which are normally measured using focused beams.

Note added in proof. Recent work of D. A. Kleinman, A. Ashkin, and G. D. Boyd (to be published) shows that, for $z_R \ll l$, maximum second-harmonic power is *not* always obtained in the index-matching direction. Although not at all apparent, this fact is contained in Eq. (54). The distinction between maximum power and the power obtained along θ_m is negligible for $z_R > \frac{1}{2}l_\alpha$. For $z_R \ll l_\alpha$, $z_R \ll l$, it is found that $(P_{2\omega})_{\max} = \pi^2 k_1^2 w_0^2$, which is a factor of 4 larger than Eq. (45); the difference occurs because in this asymptotic region there is a discontinuity in Eq. (54) at $\phi = 0$. The main purpose of this paper is to describe optimum focusing; the equations derived here are valid in crystals having $l > l_b$ for $w_0 > w_{0z}/R$. This includes the region of optimum focusing. Modifications are required to apply the ideas presented here to crystals for which $l < l_b$. The experiments were characterized by $z_R \geq 0.4l_\alpha$, and hence the calculated curves were valid.

ACKNOWLEDGMENTS

The author wishes to express his appreciation to A. E. Siegman for the many illuminating discussions they have had and for his critical reading of the manuscript. He is also indebted to S. E. Harris and G. E. Francois for their interest in this work.